Supplementary Information Appendix for "Automorphic Bloch theorems for hyperbolic lattices"

Joseph Maciejko[1,*] and Steven Rayan[2,†]

[1] *Department of Physics & Theoretical Physics Institute (TPI), University of Alberta, Edmonton, Alberta T6G 2E1, Canada*

[2] *Department of Mathematics and Statistics & Centre for Quantum Topology and Its Applications (quanTA), University of Saskatchewan, Saskatoon, Saskatchewan S7N 5E6, Canada*

[*] maciejko@ualberta.ca

[†] rayan@math.usask.ca

S1. COMPUTING THE TRANSVERSAL

As Eq. (12) in the main text makes clear, the transversal T is the set of translations g_i that tile $\mathcal{C}$ with N copies of $\mathcal{D}$. To obtain a connected cluster of given size N, we proceed as in Ref. [1], searching for group elements g_i of increasing word length L in the generators γ_j of Γ, where L is defined as the smallest possible number of generators appearing in the product expressing g_i. The set of (inequivalent) words of given L in Γ, at least for small L, can be obtained by brute-force computational enumeration and elimination of redundancies using the $PSU(1,1)$ representation of the γ_j [1]. For L up to 3, we have verified that the number of inequivalent words thus obtained matches the growth function of Γ, which can be computed directly in GAP (i.e., the number of distinct elements of smallest word length L). The unique word of length 0 is the identity $e = g_1$, which we canonically take to be the first element of T. The 8 words of length 1 are the four generators γ_j and their inverses γ_j^{-1}, which when acting on $\mathcal{D}$, produce 8 octagons adjacent to the 8 sides of $\mathcal{D}$. The 56 words of length 2 form an inequivalent subset of the 64 possible products of two words of length 1. As the computational results presented in this work are limited to clusters of size $N \leqslant N_{\max} = 25$, we can choose to limit our search to connected clusters for which words of length 3 and longer do not appear in the transversal. Though smaller than the total number of possible PBC clusters of a given size N, our results indicate that such clusters can be found at every $N \leqslant N_{\max}$, which is sufficient to illustrate our ideas. To summarize, the transversal for a cluster of size $N_{\max}$ takes the form:

$$T = \{e, \gamma_1, \ldots, \gamma_4, \gamma_1^{-1}, \ldots, \gamma_4^{-1}, g_9, \ldots, g_{N_{\max}}\}, \tag{S1}$$

where $g_9, \ldots, g_{N_{\max}}$ are length-2 words. For a cluster of size $10 \leqslant N \leqslant N_{\max}$, only $N-9$ words of length 2 are kept. For a cluster of size $2 \leqslant N \leqslant 9$, only $N-1$ words of length 1 are kept. Finally, there is only one cluster of size $N = 1$, $\mathcal{C} = \mathcal{D}$, corresponding to $\Gamma_{\text{PBC}} = \Gamma$.

S2. CLUSTERS OF PRIME ORDER

The number NSG_p of normal subgroups of prime index $N = p$ obeys a simple relation, Eq. (13) in the main text:

$$\text{NSG}_p = \frac{p^r - 1}{p - 1} = 1 + p + \ldots + p^{r-1}, \tag{S2}$$

where $r = 4$. As Fig. 3 in the main text illustrates (compare blue circles and green line), this relation does not hold for nonprime values of N.

Relation (S2) can be derived as follows. A normal subgroup $\Gamma_{\text{PBC}} \triangleleft \Gamma$ of prime index p is the kernel of the quotient homomorphism $f : \Gamma \to \Gamma/\Gamma_{\text{PBC}}$, where $\Gamma/\Gamma_{\text{PBC}}$ is a finite group of order p. Since p is prime, $\Gamma/\Gamma_{\text{PBC}}$ is isomorphic to the cyclic group $\mathbb{Z}_p$, the additive group of integers mod p. Now f is surjective, thus the number of normal subgroups of prime index p corresponds to the

number of distinct surjective homomorphisms $f : \Gamma \to \mathbb{Z}_p$. More precisely, two such maps that differ by composition with an automorphism of $\mathbb{Z}_p$ have the same kernel, thus we need to divide this number by the number $p-1$ of automorphisms of $\mathbb{Z}_p$. Since $\mathbb{Z}_p$ is abelian, f factors through the abelianization $\Gamma \to \Gamma/[\Gamma,\Gamma] \cong \mathbb{Z}^r$ of Γ, where $r = 2g = 4$ for the Bolza lattice. There are p^r homomorphisms from $\mathbb{Z}^r$ to $\mathbb{Z}_p$, obtained by assigning one of the p elements of $\mathbb{Z}_p$ to each of the r linearly independent generators of $\mathbb{Z}^r$. For p prime, this homomorphism is surjective unless each generator is mapped to the identity in $\mathbb{Z}_p$. Thus there are $p^r - 1$ surjective homomorphisms f. As said before, $\mathbb{Z}_p$ has $p-1$ automorphisms. Thus the number of distinct normal subgroups of Γ is $(p^r-1)/(p-1)$.

An interesting physical consequence of this analysis is that PBC clusters with a prime number p of unit cells are necessarily abelian, with a residual translation group isomorphic to $\mathbb{Z}_p$. Since by Euclid's theorem, prime numbers form an infinite sequence, this produces an infinite sequence of "prime PBC clusters" for which $U(1)$ hyperbolic band theory holds exactly.

S3. TRANSLATION MATRICES

We now show that the translation matrices, Eq. (26) in the main text, form a faithful representation of $\Gamma/\Gamma_{\rm PBC}$ and commute with the hopping matrix H. Using the group multiplication law [2] in $\Gamma/\Gamma_{\rm PBC}$, i.e., $[g][g'] = [gg']$, it is easily checked that Eq. (26) forms a representation of this group,

$$\begin{aligned}\Big(\mathcal{U}([g_k])\mathcal{U}([g_{k'}])\Big)_{i\ell} &= \sum_j \mathcal{U}_{ij}([g_k])\mathcal{U}_{j\ell}([g_{k'}]) \\ &= \sum_j \delta_{[g_i],[g_k g_j]}\delta_{[g_j],[g_{k'}g_\ell]} \\ &= \delta_{[g_i],[g_k g_{k'} g_\ell]} \\ &= \mathcal{U}_{i\ell}([g_k g_{k'}]),\end{aligned} \tag{S3}$$

for any two $[g_k], [g_{k'}] \in \Gamma/\Gamma_{\rm PBC}$. As pointed out in *Nonabelian clusters: a nonabelian Bloch theorem* in the main text, those matrices form the regular representation of $\Gamma/\Gamma_{\rm PBC}$. The regular representation is a faithful representation.

Finally, translation symmetry on the finite cluster is the statement that the translation operators $\mathcal{T}_{[g_k]}$ commute with $\mathcal{H}_{\rm PBC}$ for all $[g_k] \in \Gamma/\Gamma_{\rm PBC}$. For this to hold, the translation matrices $\mathcal{U}([g_k])$ must commute with the hopping matrix H. Noting that Eq. (26) is a permutation matrix, and

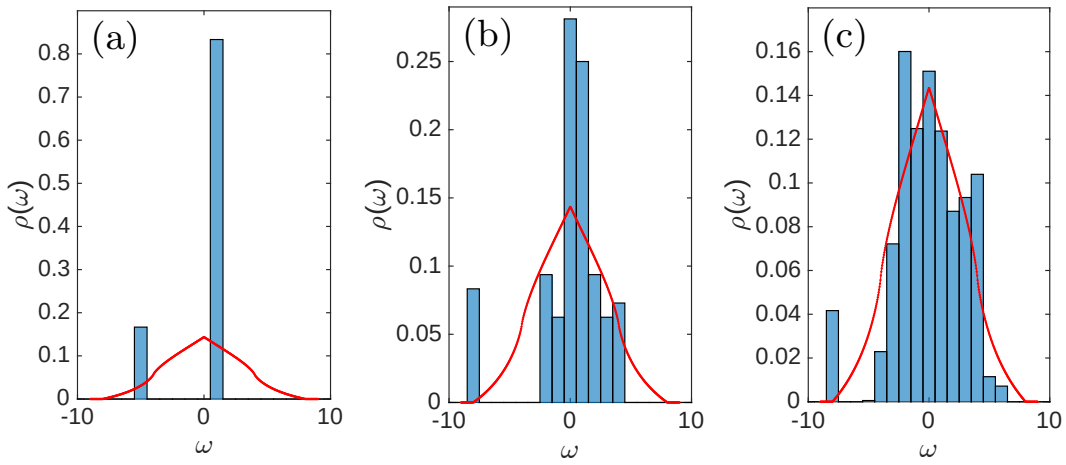

FIG. S1. Density of states histograms (blue) for abelian PBC clusters of size (a) $N = 6$, (b) $N = 12$, and (c) $N = 24$, compared with the exact density of states of a tight-binding model with unit nearest-neighbor amplitude on an infinite four-dimensional hypercubic lattice (red).

thus orthogonal, we have

$$\begin{aligned}\left(\mathcal{U}^{-1}([g_k])H\mathcal{U}([g_k])\right)_{im} &= \sum_{j\ell}\mathcal{U}_{ji}([g_k])H_{j\ell}\mathcal{U}_{\ell m}([g_k]) \\ &= -\sum_{\alpha}\sum_{j\ell}\delta_{[g_j],[g_k g_i]}\delta_{[g_\ell],[g_j\gamma_\alpha]}\delta_{[g_\ell],[g_k g_m]} \\ &= -\sum_{\alpha}\delta_{[g_k g_m],[g_k g_i\gamma_\alpha]}, \end{aligned} \tag{S4}$$

using the explicit form Eq. (24). The summand is nonzero if and only if $[g_k g_m] = [g_k g_i\gamma_\alpha]$, that is, if

$$\Gamma_{\mathrm{PBC}} g_k g_m = \Gamma_{\mathrm{PBC}} g_k g_i \gamma_\alpha. \tag{S5}$$

Multiplying on the left by g_k^{-1} and using the normality of Γ_{PBC} in Γ, we have $\Gamma_{\mathrm{PBC}} g_m = \Gamma_{\mathrm{PBC}} g_i\gamma_\alpha$, and thus

$$\left(\mathcal{U}^{-1}([g_k])H\mathcal{U}([g_k])\right)_{im} = -\sum_{\alpha}\delta_{[g_m],[g_i\gamma_\alpha]} = H_{im}. \tag{S6}$$

S4. DENSITY-OF-STATES HISTOGRAMS AND FRACTION OF ABELIAN STATES

1. Abelian clusters

To get a sense of how well $\mathrm{Jac}(\Sigma_2)$ is sampled upon increasing the PBC cluster size N, we plot in Fig. S1 density-of-states (DOS) histograms for three different cluster sizes. Here we present

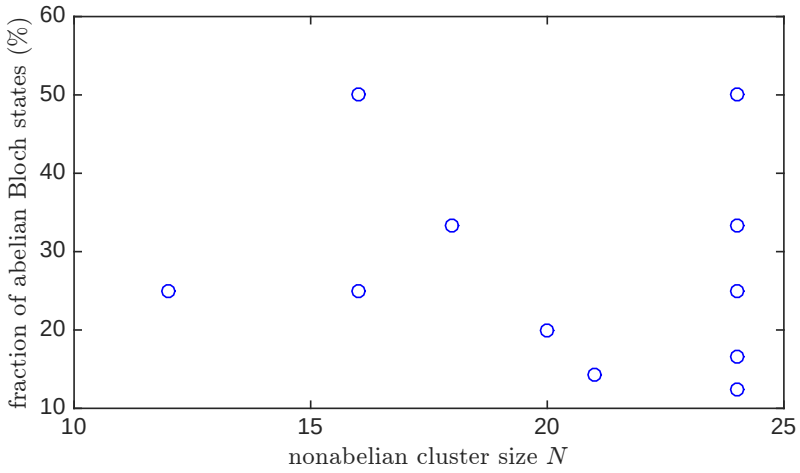

FIG. S2. Fraction $N_{\rm ab}/N$ of eigenstates obeying the abelian Bloch theorem [Eq. (27)] relative to all eigenstates, for nonabelian PBC clusters of size $N \in \{12, 16, 18, 20, 21, 24\}$.

histogram data averaged over all possible abelian clusters of a given size, to reduce finite-size effects. The finite-size histogram data can be compared with the expected DOS for an infinite abelian cluster, i.e., for the spectrum (30) in the main text but with $\boldsymbol{k} \in \mathrm{Jac}(\Sigma_2)$ a continuous variable. This corresponds to the DOS for a tight-binding model with unit nearest-neighbor hopping amplitude on the four-dimensional hypercubic lattice:

$$\rho_{\rm 4D}(\omega) = \int_{\mathrm{Jac}(\Sigma_2)} \frac{d^4k}{(2\pi)^4} \delta(\omega - E(\boldsymbol{k})). \tag{S7}$$

This can be expressed in terms of the DOS for a nearest-neighbor tight-binding model on the simple cubic lattice,

$$\rho_{\rm 4D}(\omega) = \int_{-\pi}^{\pi} \frac{dk_4}{2\pi} \rho_{\rm 3D}(\omega + 2\cos k_4), \tag{S8}$$

which can be computed analytically:

$$\rho_{\rm 3D}(\omega) = -\frac{1}{\pi} \,\mathrm{Im}\left[\frac{1}{\omega + i\eta} P\left(\frac{6}{\omega + i\eta}\right)\right], \tag{S9}$$

where η is a positive infinitesimal, and we define [3]:

$$P(y) = \frac{\sqrt{1 - \frac{3}{4}x_1}}{1 - x_1} \left(\frac{2}{\pi}\right)^2 K(k_+^2) K(k_-^2), \tag{S10}$$

$$k_\pm^2 = \frac{1}{2} \pm \frac{1}{4} x_2 \sqrt{4 - x_2} - \frac{1}{4}(2 - x_2)\sqrt{1 - x_2}, \tag{S11}$$

$$x_2 = \frac{x_1}{x_1 - 1}, \tag{S12}$$

$$x_1 = \frac{1}{2} + \frac{1}{6}y^2 - \frac{1}{2}\sqrt{(1 - y^2)\left(1 - \frac{1}{9}y^2\right)}, \tag{S13}$$

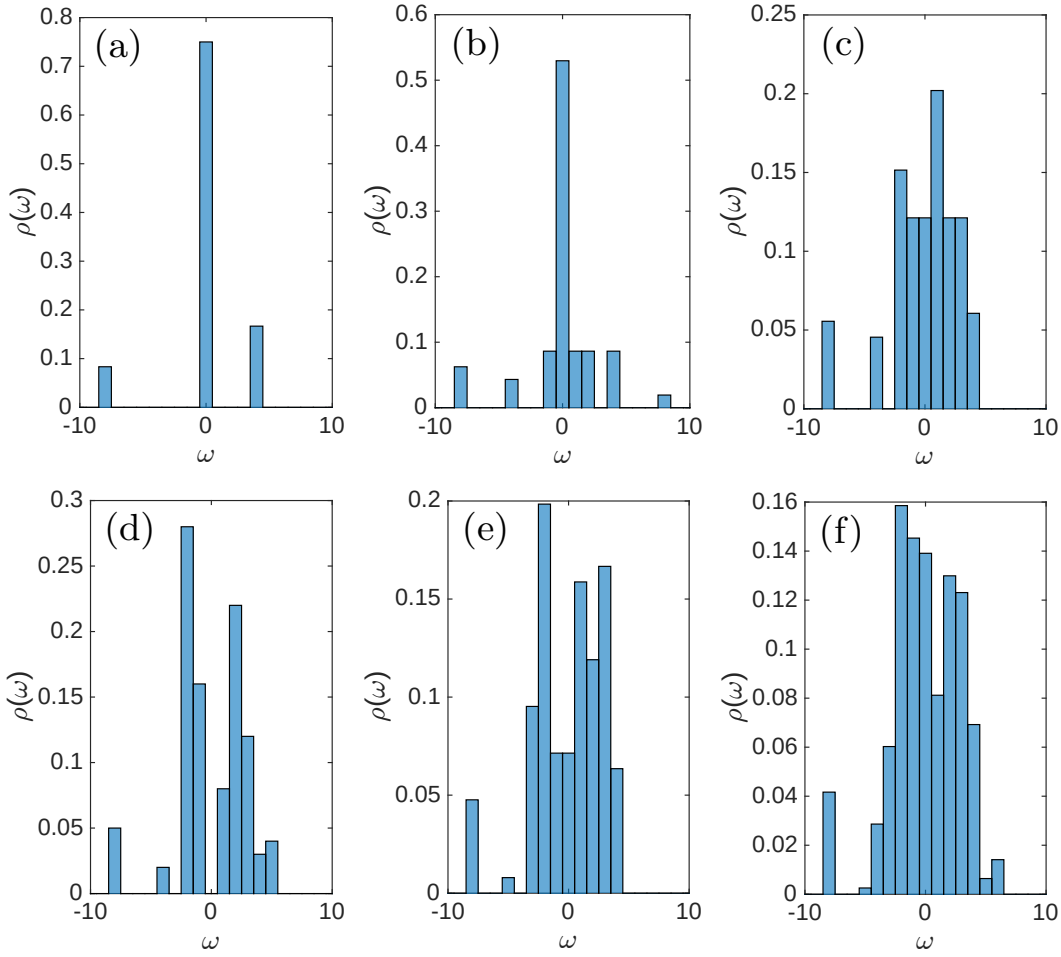

FIG. S3. Density of states histograms for nonabelian PBC clusters of size (a) $N = 12$, (b) $N = 16$, (c) $N = 18$, (d) $N = 20$, (e) $N = 21$, and (f) $N = 24$.

and $K(m)$ is the complete elliptic integral of the first kind:

$$K(m) = \int_0^{\pi/2} \frac{d\theta}{\sqrt{1 - m \sin^2 \theta}}. \tag{S14}$$

The remaining integral over k_4 in Eq. (S8) can be performed numerically. It is clear from Eqs. (30) and (S7) that the DOS vanishes for ω outside the interval $[-8, 8]$. We see from Fig. S1 that as N increases, the finite-size DOS histograms approximate the exact DOS increasingly well.

2. Nonabelian clusters

For a given nonabelian cluster, the fraction N_{ab}/N of abelian states among all eigenstates can be determined from the number $\mathcal{N}_{\mathrm{1D}}$ of one-dimensional irreps of $\Gamma/\Gamma_{\mathrm{PBC}}$, which can be computed using representation-theoretic routines in GAP. Indeed, since each one-dimensional irrep

occurs only once in the direct-sum decomposition (32) in the main text, we have $N_{\rm ab} = \mathcal{N}_{\rm 1D}$. In Fig. S2, we plot for each cluster size $N \in \{12, 16, 18, 20, 21, 24\}$ the distinct values of $N_{\rm ab}/N$ found across all possible nonabelian clusters of size N. As the cluster size increases, the minimum value of $N_{\rm ab}/N$ appears to decrease, which suggests higher-dimensional representations play an increasingly important role for larger clusters. However, for the largest system size considered, nonabelian clusters can nonetheless still be found for which up to 50% of the spectrum consists of abelian states. Interestingly, the averaged DOS histograms for nonabelian clusters (Fig. S3) are qualitatively not too dissimilar from those for abelian clusters (Fig. S1), despite the presence of a substantial fraction of nonabelian states. The reason for this unexpected similarity is not presently understood and deserves further investigation.

The observations above, combined with the fact that nonabelian clusters only appear at certain values of N, lead us to conjecture that nonabelian clusters are those that exhibit a higher degree of symmetry than their abelian counterparts. In exact diagonalization studies of quantum Hamiltonians on ordinary Euclidean lattices, certain high-symmetry points in the Brillouin zone will be excluded by an anisotropic choice of cluster geometry. Likewise here, the relative fraction of abelian to nonabelian "Brillouin zones" appearing in the spectrum can be tuned by changing the geometry of the cluster, to the point of completely excluding nonabelian representations for certain system sizes.

S5. IRREP DECOMPOSITION FOR A NONABELIAN CLUSTER

For the chosen nonabelian PBC cluster of size $N = 24$, the irreducible character table of the finite group $\Gamma/\Gamma_{\rm PBC}$ of order 24, computed by GAP, is shown in Table S1. The number of conjugacy classes/irreps is found to be $\mathcal{N} = 12$. The first row of Table S1 denotes the label $C = 1, \ldots, \mathcal{N}$ of the conjugacy class, and the second, the number n_C of group elements in each class. One can check explicitly that the characters $\chi^{(\lambda)} = \operatorname{tr} D^{(\lambda)}$ of the irreps $\lambda = 1, \ldots, \mathcal{N}$, which depend only on the class C, satisfy the properties of row orthogonality,

$$\sum_{C=1}^{\mathcal{N}} n_C \chi^{(\lambda)}(C)^* \chi^{(\lambda')}(C) = N \delta_{\lambda\lambda'}, \tag{S15}$$

and column orthogonality,

$$\sum_{\lambda=1}^{\mathcal{N}} \chi^{(\lambda)}(C)^* \chi^{(\lambda)}(C') = \frac{N}{n_C} \delta_{CC'}, \tag{S16}$$

where $N = 24$ is the order of the group [4]. The first column of the table corresponds to the dimension $r_\lambda = \chi^{(\lambda)}(e)$ of irrep λ; thus this group has 8 one-dimensional irreps $\lambda = 1, \ldots, 8$ and 4 two-dimensional irreps $\lambda = 9, \ldots, 12$.

C	1	2	3	4	5	6	7	8	9	10	11	12
n_C	1	1	1	1	2	2	2	2	3	3	3	3
$D^{(1)}$	1	1	1	1	1	1	1	1	1	1	1	1
$D^{(2)}$	1	1	1	1	1	1	1	1	-1	-1	-1	-1
$D^{(3)}$	1	-1	a	$-a$	1	-1	a	$-a$	c	$-c$	$-1/c$	$1/c$
$D^{(4)}$	1	-1	a	$-a$	1	-1	a	$-a$	$-c$	c	$1/c$	$-1/c$
$D^{(5)}$	1	-1	$-a$	a	1	-1	$-a$	a	$-1/c$	$1/c$	c	$-c$
$D^{(6)}$	1	-1	$-a$	a	1	-1	$-a$	a	$1/c$	$-1/c$	$-c$	c
$D^{(7)}$	1	1	-1	-1	1	1	-1	-1	a	a	$-a$	$-a$
$D^{(8)}$	1	1	-1	-1	1	1	-1	-1	$-a$	$-a$	a	a
$D^{(9)}$	2	2	-2	-2	-1	-1	1	1	0	0	0	0
$D^{(10)}$	2	2	2	2	-1	-1	-1	-1	0	0	0	0
$D^{(11)}$	2	-2	b	$-b$	-1	1	$-a$	a	0	0	0	0
$D^{(12)}$	2	-2	$-b$	b	-1	1	a	$-a$	0	0	0	0

TABLE S1. Character table of $\Gamma/\Gamma_{\rm PBC}$ for the $N = 24$ nonabelian cluster considered in *Irrep decomposition of the finite-size spectrum: an explicit example*. Here $a = -i$, $b = -2i$, and $c = e^{-i\pi/4}$. C denotes the conjugacy class, n_C the number of group elements in each class, and $D^{(\lambda)}$ the 12 irreps labeled by $\lambda = 1, \ldots, 12$.

To determine to which irrep each Bloch eigenstate of the cluster belongs, we construct projector matrices [4],

$$\Pi^{(\lambda)} = \frac{r_\lambda}{N} \sum_{[g_k]\in\Gamma/\Gamma_{\rm PBC}} \chi^{(\lambda)}([g_k])^* \mathcal{U}([g_k]), \tag{S17}$$

which obey $\Pi^{(\lambda)}\Pi^{(\lambda')} = \delta_{\lambda\lambda'}\Pi^{(\lambda)}$ and project an arbitrary state $\psi(z_i)$ onto irrep λ. Since the $\Pi^{(\lambda)}$ are linear combinations of translation matrices $\mathcal{U}$, they commute with H and can thus be simultaneously diagonalized with it. Finally, we note that the eigenvalues of $\Pi^{(\lambda)}$ can only be 1 or 0, and that an eigenstate of H can have a $\Pi^{(\lambda)}$-eigenvalue of 1 for only a single $\Pi^{(\lambda)}$. Such an eigenstate $\psi^{(\lambda)}_\mu$ thus necessarily belongs to irrep λ of $\Gamma/\Gamma_{\rm PBC}$.

S6. GEOMETRY OF HIGHER-RANK MODULI SPACES

In this section, we provide further information on the geometry of the rank-r moduli spaces for general r. While a positively-curved $SU(r)$ fibre is a feature of these moduli spaces in general—in algebro-geometric language, $\mathcal{M}(\Sigma_g, SU(r))$ is *Fano*, as opposed to tori which are *Calabi–Yau*—we also caution that the $g = r = 2$ example is rather unusual in that (a) the moduli space happens to be globally smooth and (b) the geometry of the moduli space is known in an exact

way. If we let $\mathcal{M}(\Sigma_g, U(r), d)$ denote the moduli space of semistable rank-r holomorphic vector bundles with first Chern class $c_1(V) = d$, then it is worth noting that the moduli space is only guaranteed to be smooth when r and d are coprime [5]. In the coprime case, it is impossible to achieve equality in the stability inequality, and so the potentially singular points disappear from the moduli space. In our case of $\mathcal{M}(\Sigma_g, U(r)) = \mathcal{M}(\Sigma_g, U(r), 0)$, this coprimality never occurs and we do have bundles for which equality is achieved, which makes the global smoothness of $\mathcal{M}(\Sigma_2, U(2))$ somewhat surprising. In terms of $\pi_1(\Sigma_g)$-representations, coprimality of r and d means that we may construct a compact character variety from irreps alone; however, the nonzero first Chern class must be incorporated and manifests as a twist by a nontrivial root of unity in the defining relation of the character variety. For our purposes, we will restrict to the $d = 0$ case, in which case we have the ordinary character variety as the rank-r component of the space of crystal momenta.

Physically, one can still prescribe meaning to $\mathcal{M}(\Sigma_g, U(r))$ as a space of higher-dimensional fluxes, but the (co)homologies of the $\mathcal{M}(\Sigma_g, U(r))$—in particular the relations that intertwine cycles—are far more involved now than that of $\mathrm{Jac}(\Sigma_g)$. We note, however, that there is a natural map $\mathcal{M}(\Sigma_g, U(r)) \to \mathrm{Jac}(\Sigma_g)$ obtained by $V \mapsto \det(V)$, where $\det(V)$ is the line bundle whose transition functions are the determinants of those of V. In other words, there is an algebraic projection of higher-dimensional fluxes onto the magnetic fluxes in the abelian Brillouin zone.

S7. EXPERIMENTAL PROPOSAL

In this last section, we provide further details of the proposal outlined in *Summary and outlook* to realize hyperbolic abelian/nonabelian Bloch states in CQED and/or electric circuit network experiments. Figure 9 in the main text is reproduced in enlarged format as Fig. S4; close-ups of the boundary octagons A, B, C (green) are given in Fig. S5.

To engineer PBC that are consistent with the normal subgroup structure discussed in the main text, the 88 boundary sites must be wired together in particular ways. In Tables S2 and S3, we list the 74 distinct bonds between boundary sites i and $j > i$ that must be established to engineer (a particular choice of) abelian and nonabelian PBC, respectively. This information is also included in the SI files Dataset 1 and Dataset 2, respectively, where the first (second) column corresponds to the value of i (j). The hopping strength (capacitive coupling) must be the same for those boundary bonds as for the intra-cluster bonds (red nearest-neighbor bonds in Figs. S4 and S5) in order to preserve Fuchsian translation symmetry and the automorphic Bloch theorem. With either abelian or nonabelian PBC, both bulk and boundary sites are connected to 3 nearest neighbors (as can be checked from Tables S2-S3), again consistent with translation symmetry on the $\{8, 3\}$ lattice.

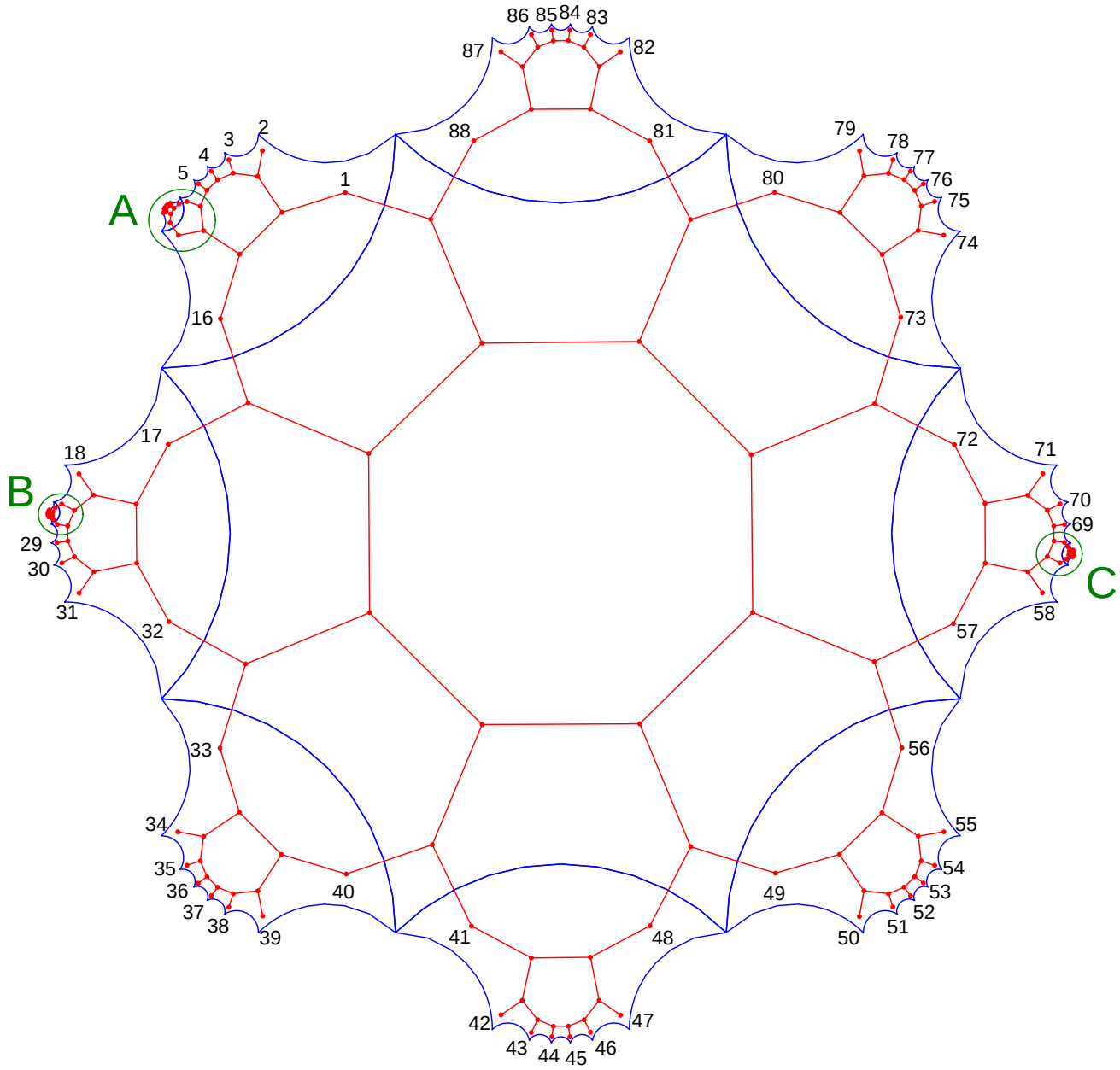

FIG. S4. Proposed realization of abelian/nonabelian Bloch states using CQED or electric circuit implementations (enlarged version of Fig. 9 in the main text). A cluster of 192 sites (red vertices) of the $\{8, 3\}$ lattice corresponds to $N = 12$ Bolza unit cells (blue octagons) with 16 sites each. Close-ups of the A, B, C boundary octagons (green) are given in Fig. S5. The 88 boundary sites can be wired together in two different ways to achieve either abelian PBC (Table S2) or nonabelian PBC (Table S3).

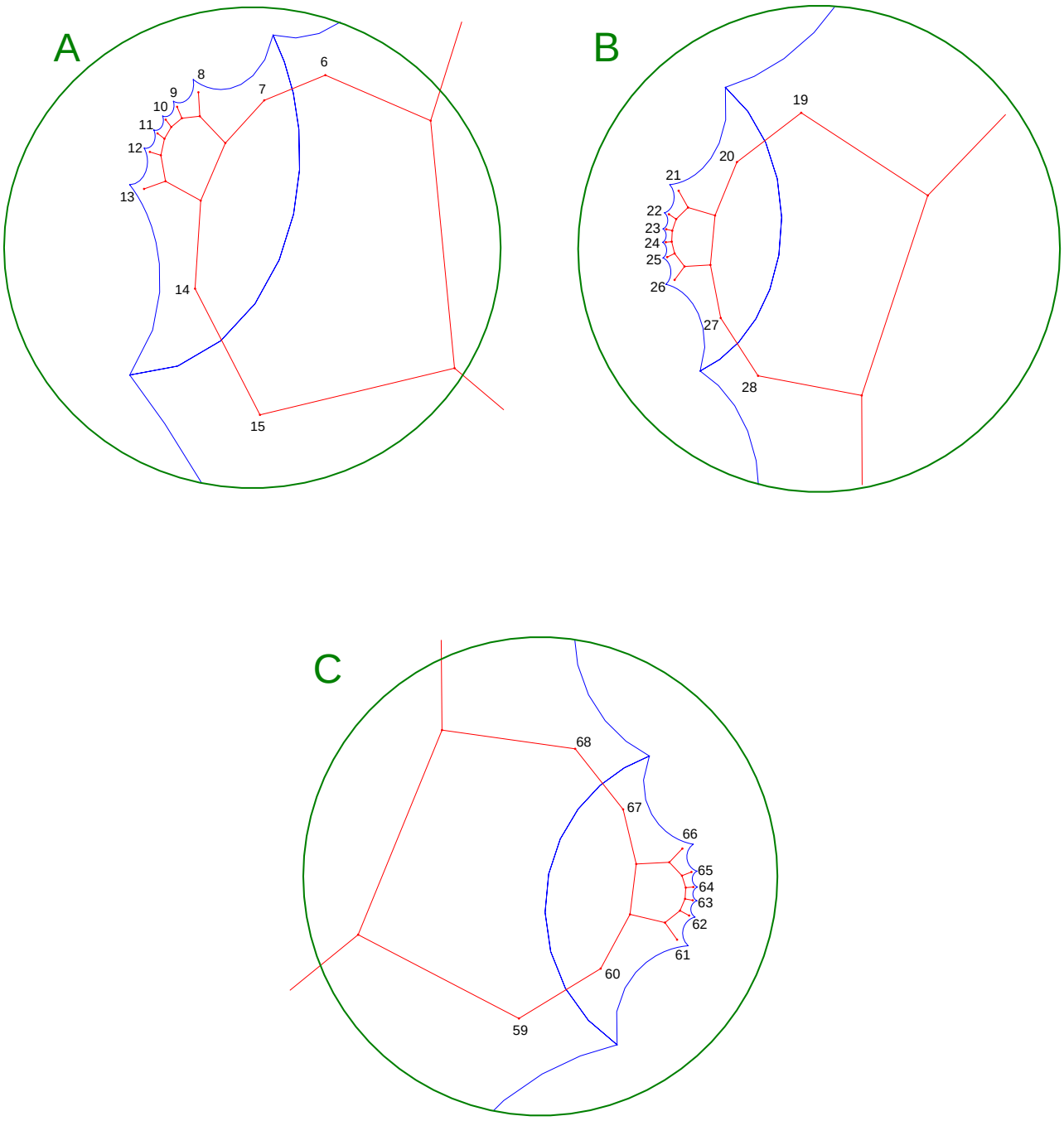

FIG. S5. Close-ups of the A, B, C boundary octagons in Fig. S4.

i	j	i	j	i	j	i	j
1	36	14	86	29	68	44	71,76
2	30,35	15	67	30	85	45	70
3	29,52	16	66	31	79,84	49	76
4	46,51	17	62	32	78	50	70,75
5	21,45	18	61	33	63	51	69
6	20	21	58	34	62	52	86
7	59	22	57,74	36	84	53	61,85
8	58,75	23	73,82	37	78,83	54	60
9	47,74	24	40,81	38	72,77	64	80
10	46,55	25	39,48	39	71	65	79,88
11	19,54	26	47,56	41	64	66	87
12	18,35	27	55	42	63,83		
13	34,87	28	69	43	77,82		

TABLE S2. List of connections among boundary sites i and j of $\{8,3\}$ cluster of Fig. S4 to engineer abelian PBC (data also included in Dataset 1).

i	j	i	j	i	j	i	j
1	43	14	86	28	69	45	79,84
2	30,42	15	23	29	68	46	61,78
3	29,38	16	22	30	78	47	60
4	37,53	18	63	31	77,86	49	76
5	52,65	19	62	32	85	50	75,84
6	64	20	80	34	64	51	71,83
7	59	21	58,79	35	63,83	52	70
8	58,75	22	57	36	77,82	54	62
9	40,74	23	82	37	76	55	61
10	18,39	24	54,81	38	72	65	88
11	17,56	25	48,53	39	71	66	74,87
12	42,55	26	34,47	43	70	67	73
13	41,87	27	33	44	69,85		

TABLE S3. List of connections among boundary sites i and j of $\{8,3\}$ cluster of Fig. S4 to engineer nonabelian PBC (data also included in Dataset 2).

[1] I. Boettcher, A. V. Gorshkov, A. J. Kollár, J. Maciejko, S. Rayan, and R. Thomale, "Crystallography of Hyperbolic Lattices," arXiv:2105.01087 (2021).

[2] The set of cosets of a *normal* subgroup H in a group G indeed form a group, since for any $g, g' \in G$, we have $[g][g'] = (Hg)(Hg') = H(gHg^{-1})gg' = Hgg' = [gg']$.

[3] G. S. Joyce, "Lattice Green function for the simple cubic lattice," J. Phys. A: Gen. Phys. **5**, L65–L68 (1972).

[4] M. Tinkham, *Group Theory and Quantum Mechanics* (McGraw-Hill, New York, 1964).

[5] M. S. Narasimhan and C. S. Seshadri, "Stable and Unitary Vector Bundles on a Compact Riemann Surface," Ann. Math. **82**, 540–567 (1965).